Soliton dynamics in new models with parametrized periodic double-well and asymmetric substrate potentials

M. Remoissenet
Laboratoire d'Optique du Réseau Cristallin (ORC), Faculté des Sciences, Université de Dijon 6 boulevard Gabriel, F-21100 Dijon, France

M. Peyrard
*Center for Nonlinear Studies, Los Alamos National Laboratory, Los Alamos, New Mexico 87545 and Laboratoire d'Optique du Réseau Cristallin (ORC), Faculté des Sciences, Université de Dijon, 6 boulevard Gabriel, F-21100 Dijon, France**

(Received 6 May 1983)

A chain of atoms, harmonically coupled, subjected to a new type of parametrized substrate potential is studied in the strong coupling limit. We consider in particular two cases in which the shape of the potential can be moved in a controlled manner from the simply periodic and symmetrical sine-Gordon model to doubly periodic potentials: a periodic double-well deformable potential (DWDP) and an asymmetrical deformable potential (ASDP). Kinks solutions are calculated analytically in the continuum limit. In the DWDP case two types of symmetric kinks with different masses are obtained. In this model the numerical studies of kink-kink and kink-antikink collisions show that kinks properties are very close to those of an integrable system. Consequently, the collisions are well described by treating the excitations as relativistic quasiparticles if conversion between the two types of particles is taken into account. In the ASDP case, two types of asymmetric kinks with identical masses are found. Owing to this asymmetry, the interaction between two excitations depends on the side of the kinks which first comes into contact during the collision, and this "polarization" of the kinks introduces new features when they collide. Moreover, these kinks interpolate between two ground states which do not have the same phonon spectrum. In some cases small-amplitude oscillations can be trapped between a kink and an antikink and induce a new type of resonant interaction between them. In addition, in the search for breather solutions as the low-amplitude limit of nonlinear Schrödinger envelope solitons, necessary conditions for the existence of breather modes are determined analytically and confirmed numerically.

I. INTRODUCTION

Nonlinear solitonlike excitations in one dimensional physical systems have recently attracted considerable attention.[1] A standard model[2] in condensed matter physics is the discrete Frenkel-Kontorova (FK) or sine-Gordon[2] (SG) chain, which consists of a chain of atoms connected with harmonic springs, interacting with a sinusoidal substrate potential. In the continuum limit it becomes the SG model,[3] an integrable model[4] of exceptional mathematical interest with "strict soliton" solutions. However, in real systems, as for instance Josephson junctions, incommensurate systems, charge-density wave condensates, or crystals with dislocations, the shape of the potential can deviate strongly from a sinusoidal one. In that context, introducing a one-dimensional model[5] with nonlinear periodic deformable potential, we have recently shown[6] that the shape of the substrate potential is a factor of particular importance when modeling physical systems. Discreteness effects and the related soliton pinning increase with the deformation of the potential. When this parametrized potential is used in a generalized FK model[7] to describe incommensurate phases, the critical amplitude of the potential above which the incommensurate structure becomes pinned to the substrate and the phason mode disappears (transition by "breaking of analyticity"), is considerably lowered. Moreover, the model[5,6] shows a very rich phenomenology[8] for the resonant collisions of nonlinear excitations in nonintegrable theories. Very recently it has been shown[9] that these collisions can generate chaotic states in this nonintegrable model with infinite degrees of freedom.

Encouraging as these results are, they are nevertheless somewhat limited in their applicability to real physical systems by the fact that the potential considered above, although deformable, is periodic and possesses only one type of potential barrier which is symmetrical and therefore can support only one type of kink solution (a kink being a solitonlike excitation in which the relevant field evolves across a barrier from one minimum to an adjacent minimum). For wider generality it is desirable[10] to have a model that describes a "polykink system" (i.e., one for which more than one type of solitonic excitation is possible) with symmetric or asymmetric kink solutions.

In this paper we introduce a new family of nonlinear periodic deformable potentials which generalizes the model previously considered[5,6]

$$V(\phi,r)=A(r)\frac{1+e\cos\phi}{[1+r^2+2r\cos(\phi/m)]^p}\ , \tag{1.1}$$

where r is a shape parameter with range $-1<r<1$, $A(r)$ is a normalizing amplitude function; m,p are integers and $e=\pm 1$. The potentials defined by Eq. (1.1) reduce to the familir SG potential through a continuous deformation when the parameter r goes to zero. With $A(r)=(1-r)^2$, $m=p=1$, $e=-1$ one recovers the potential recently studied.[6] For $A(r)=(1-r^2)^2$, $m=p=2$, $e=-1$, $0<r<1$, one obtains an asymmetric deformable potential (ASDP) with a constant barrier height equal to 2, represented in Fig. 1(a) for different values of r; the position ϕ_b of the potential barrier depends on r and is determined by $\cos(\phi_b/2)=2r/(1+r^2)$; two successive wells are inequivalent with, respectively, a flat and a sharp bottom. For $A(r)=(1-r)^4$, $m=p=2$, $e=+1$, $0<r<1$, one gets a double-well deformable potential (DWDP), plotted in Fig. 1(b). At $\phi=0$ the height of the barrier separating two double wells is equal to 2. Thus in the two particular cases defined above one can move in a controlled manner from the simply periodic and symmetric SG model (which is completely integrable[4]) to doubly periodic or asymmetric periodic models which are not completely integrable. With an adequate choice of the parameters one can also obtain from Eq. (1.1) a very rich variety of many other deformable potentials (as for instance symmetric or asymmetric multiple-well potentials) with related soliton solutions which allow the modeling of many different specific physical situations without employing perturbation methods.

In this paper we present the important and interesting new features which emerge from the parallel study of the DWDP and ASDP systems defined above: both of them possess two kinds of solitonlike excitations but with completely different properties. The organization of the paper is as follows. In Sec. II the kink solutions of the equations of motions are calculated exactly. The existence of breather solutions is studied approximately in the low amplitude limit. Section III is devoted to the numerical studies of the solitonlike excitations. We investigate particulary their stability and particlelike interactions between the two types of kinks, including breather formation in kink-antikink collisions. For the ASDP case resonant interactions are studied. Section IV gives a brief summary and discussion.

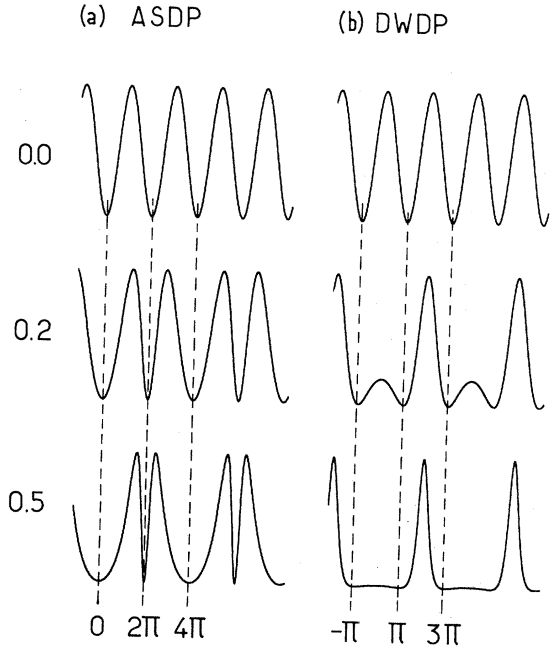

FIG. 1. Representation of the potentials $V(\phi,r)$ (a) for the ASDP model and (b) DWDP model for different values of the shape parameter r.

II. EQUATIONS OF MOTION AND ANALYTICAL SOLUTIONS

A. Kink excitations

We consider an array of atoms of mass m connected with harmonic springs interacting with the periodic "on-site" potential $V(\phi,r)$ with period $a=4\pi$. The potentials defined in Sec. I and represented in Figs. 1(a) and 1(b) are given by

$$V(\phi,r)=\begin{cases}\dfrac{(1-r^2)^2(1-\cos\phi)}{(1+r^2+2r\cos\frac{1}{2}\phi)^2} & \text{for ASDP} \quad (2.1)\\ \dfrac{(1-r)^4(1+\cos\phi)}{(1+r^2+2r\cos\frac{1}{2}\phi)^2} & \text{for DWDP} . \quad (2.2)\end{cases}$$

For $r=0$ one recovers in each case the SG potential.

The Hamiltonian is

$$H=\sum_i aA\left[\tfrac{1}{2}\dot{\phi}_i^2+\frac{1}{2}\frac{C_0^2}{a^2}(\phi_{i+1}-\phi_i)^2+\omega_0^2V(\phi_i,r)\right], \quad (2.3)$$

where ϕ_i is the scalar dimensionless displacement of the ith atom. The constant C_0 is a characteristic velocity, ω_0 a characteristic frequency, $d=C_0/\omega_0$ defines the discreteness parameter and the factor $A=ma$ sets the energy scale. In the continuum or "displacive" limit ($d\gg 1$), the Hamiltonian (2.3) of the system reduces[6] to a generalized Klein-Gordon Hamiltonian

$$H=A\int dx\,[\tfrac{1}{2}\phi_t^2+\tfrac{1}{2}C_0^2\phi_x^2+\omega_0^2V(\phi,r)] , \quad (2.4)$$

where $\phi(x,t)$ is a one-component field variable and $\phi_x=\partial\phi/\partial x$ replaces $(\phi_{i+1}-\phi_i)/a$. Topologically stable single kink or quasisoliton solutions will then follow[3,6,11] from the associated equation of motion for ϕ

$$\phi_{tt}-C_0^2\phi_{xx}+\omega_0^2\frac{\partial V(\phi,r)}{\partial\phi}=0 . \quad (2.5)$$

We simply look for traveling wave solutions and apply boundary conditions for a kink, ϕ, with velocity v: With the use of $s=x-vt$ the implicit solution describing a single kink is[6]

$$\frac{\gamma s}{d}=\pm\frac{1}{\sqrt{2}}\int_{\phi(0)}^{\phi(s)}d\phi[V(\phi,r)]^{-1/2} \quad (2.6)$$

where $\gamma=(1-v^2/C_0^2)^{-1/2}$. The energy associated with a single kink at rest is given by

$$E_K^0=M_KC_0^2 , \quad (2.7)$$

where M_K is the kink rest mass given by

TABLE I. Various quantities of the ASDP and DWDP systems associated with the kink (+) and antikink (−) solution of Eq. (2.5). The rest masses M_{K_1} and M_{K_2} are expressed in terms of $M_{K_0}=8A/d$, the SG soliton rest mass.

$V(\phi,r)$	ASDP	DWDP
$\frac{\gamma s_1}{d}$	$\frac{1+r^2}{1-r^2}\ln\left[\tan\left[\frac{\phi}{4}\right]\right]+\frac{2r}{1-r^2}\ln\left[\sin\left[\frac{\phi}{2}\right]\right]$	$\frac{1+r^2}{(1-r)^2}\ln\left[\tan\left[\frac{\phi}{4}+\frac{\pi}{4}\right]\right]+\frac{r\phi}{(1-r)^2}$
$\frac{\gamma s_2}{d}$	$\frac{1+r^2}{1-r^2}\ln\left[-\cot\left[\frac{\phi}{4}\right]\right]-\frac{2r}{1-r^2}\ln\left[-\sin\left[\frac{\phi}{2}\right]\right]$	$\frac{1+r^2}{(1-r)^2}\ln\left[-\cot\left[\frac{\phi}{4}+\frac{\pi}{4}\right]\right]-\frac{4}{(1-r)^2}(\phi-2\pi)$
M_{K_1}	$M_{K_0}\frac{1-r^2}{2r}\ln\left[\frac{1+r}{1-r}\right]$	$M_{K_0}\frac{(1-r)^2}{r}\left[\frac{\pi}{4}-\frac{1+r^2}{1-r^2}\arctan\left[\frac{1-r}{1+r}\right]\right]$
M_{K_2}	$M_{K_0}\frac{1-r^2}{2r}\ln\left[\frac{1+r}{1-r}\right]$	$M_{K_0}\frac{(1-r)^2}{r}\left[-\frac{\pi}{4}+\frac{1+r^2}{1-r^2}\arctan\left[\frac{1+r}{1-r}\right]\right]$

$$M_K=\sqrt{2}\frac{A}{d}\int_{\phi_1}^{\phi_2}d\phi\,|[V(\phi,r)]^{1/2}|\ , \tag{2.8}$$

where ϕ_1 and ϕ_2 are two successive degenerate minima of $V(\phi,r)$. The relevant results listed in Table I for the ASDP and DWDP systems are now easily derived from Eqs. (2.1), (2.2), (2.6), and (2.8); as expected for $r=0$ they reduce to the SG results. For the DWDP system two types of kink solutions are calculated. For the type-I kink the ground states at $\phi=-\pi$ and $\phi=\pi$ are connected over the variable potential barrier [see Fig. 2(a)] at $\phi=0$; its rest mass M_{K_1} can vary from M_{K_0} ($r=0$) to zero ($r\to 1$). For the type-II kink the ground states at $\phi=\pi$ and $\phi=3\pi$ are connected over the constant potential barrier (equal to two); its rest mass M_{K_2} can range from M_{K_0} ($r=0$) to zero ($r\to 1$), except that for the case $r=0$ we always have $(M_{K_1}/M_{K_2})>1$. For the ASDP system two kinds of asymmetric kinks (antikinks) are obtained which correspond, respectively, to the ranges $(0,2\pi)$ and $(2\pi,4\pi)$ for ϕ. The waveforms of two successive kinks are represented in Fig. 2(b) for different values of r. Two successive kinks are antisymmetric. The masses of the kinks expressed in terms of the SG soliton rest mass $M_{K_0}=8A/d$, are equal. The asymmetry of their shapes is controlled by the parameter r: The positions s_{M_1} and s_{M_2} of their centers of mass correspond to $\phi_{M_1}=2\arccos(-r)$ and $\phi_{M_2}=4\pi-\phi_{M_1}$, quantities which are calculated from Eq. (2.8) and from the values of M_{K_1} and M_{K_2} (see Table I). For this ASDP model explicit solutions can be derived in the particular case $r=2-\sqrt{3}$. In this case we have $4r=r^2+1$ and the implicit solution given in Table I can be inverted.

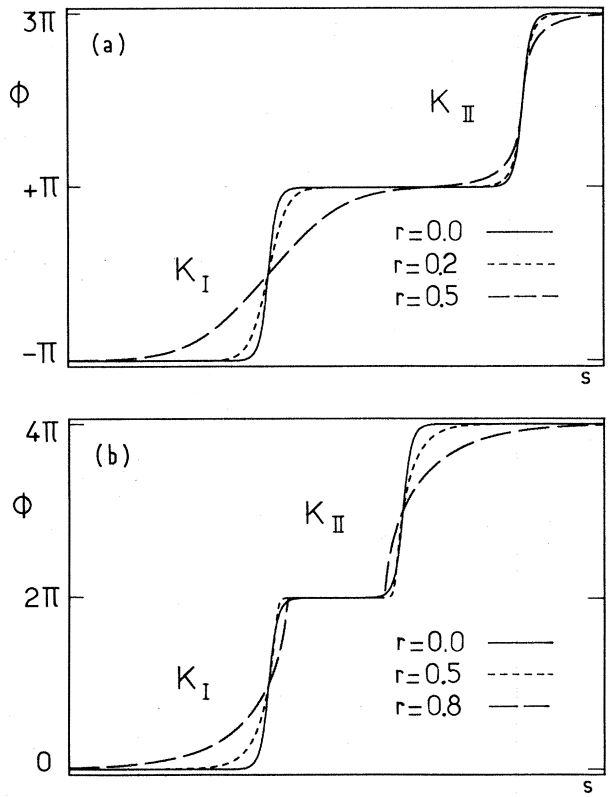

FIG. 2. Kink profiles for various values of the shape parameter r for the two models: (a) DWDP, (b) ASDP.

If we define $T=\tan(\phi_I/4)$ and

$$a=\tfrac{1}{2}\exp\left[\frac{2\sqrt{3}-3}{2-\sqrt{3}}\frac{\gamma s_1}{d}\right]$$

we obtain

$$T=\frac{a}{3}+(a)^{1/3}\left\{\left[\left[\frac{1}{2}+\frac{a^2}{27}\right]+\left[\frac{1}{4}+\frac{a^2}{27}\right]^{1/2}\right]^{1/3}+\left[\left[\frac{1}{2}+\frac{a^2}{27}\right]-\left[\frac{1}{4}+\frac{a^2}{27}\right]^{1/2}\right]^{1/3}\right\} \tag{2.9}$$

and ϕ_I is given by

$$\phi_I=4\arctan(T)\ . \tag{2.10}$$

The second solution ϕ_{II} is simply $\phi_{II}=4\pi-\phi_I$.

In the linear limit ($|\phi|\ll 1$) Eq. (2.5) reduces to the Klein-Gordon equation

$$\phi_{tt}-C_0^2\phi_{xx}+\omega_m^2\phi=0,\quad m=1,2,3\ . \tag{2.11}$$

For the ASDP system ($m=1$ or 2) two characteristic frequencies ω_1 and ω_2 can be defined (corresponding to the small phonon oscillations in the bottom of the two kinds of wells):

$$\omega_1=\omega_0\left[\frac{1-r}{1+r}\right],\quad \omega_2=\omega_0\left[\frac{1+r}{1-r}\right]. \tag{2.12}$$

Thus this system supports *two* kinds of phonon excitations and this is responsible of an interesting property of the kinks. Indeed, in order to obtain the ground state of the system we must put $\phi=0$ or $\phi=2\pi$ along the whole system. If we choose the first solution ($\phi=0$) all the atoms (or the continuum chain in the continuum limit) lie in the wells with a flat bottom and consequently the frequency of the long-wavelength phonons is ω_1. On the contrary for the second solution ($\phi=2\pi$) all atoms are in the wells with a sharp bottom and the frequency of the long-wavelength phonons is ω_2. Thus the model *has two energetically equivalent ground states* but *these two states are not physically equivalent* (in particular, they do not have the same dynamical properties—phonons frequencies). These two states may for instance represent two different phases. A kink in this model separates one ground state from the other and thus it is a wall between two different "media." To our knowledge it is the first time that this kind of kink has been investigated. This peculiarity is also of great importance for the thermodynamical properties of the system. When kinks are moving in such a system they move the boundaries between regions that do not carry the same types of phonons. The case of the DWDP system ($m=3$) is simpler since it carries only one type of phonon with a characteristic frequency

$$\omega_3=\omega_0\frac{(1-r)^2}{1+r^2}. \tag{2.13}$$

B. Breather modes in the low-amplitude limit

In contrast to Sec. II A where we exactly calculated the kink solutions, in this section we rely on the approximate breather solutions in the small-amplitude limit. It is now well known[12] that in the low-amplitude limit the SG breather mode is equivalent to a nonlinear Schrödinger (NLS) envelope soliton. Kaup and Newell have pointed out[13] that this result can be applied to a much wider class of systems with potential $V(\phi)$ different from the SG potential. This result is now used to determine the low amplitude breather solutions.

1. ASDP model

For the ASDP model the small nonlinear oscillations correspond to oscillations in the bottom of one of the two wells of the potential: $\phi\to\epsilon\Phi_1$ or $\phi\to\epsilon\Phi_2+2\pi$ with $\epsilon\ll 1$. For these two cases inserting Eq. (2.1) in Eq. (2.5) and expanding in terms of Φ gives

$$\Phi_{1tt}-C_0^2\Phi_{1xx}+\omega_1^2\left[\Phi_1-\epsilon^2\frac{1+r^2-4r}{(1+r)^2}\frac{\Phi_1^3}{6}\right]=0 \tag{2.14a}$$

for $\Phi\to\epsilon\Phi_1$, and

$$\phi_{2tt}-C_0^2\Phi_{2xx}+\omega_2^2\left[\Phi_2-\epsilon^2\frac{1+r^2+4r}{(1-r)^2}\frac{\Phi_2^3}{6}\right]=0 \tag{2.14b}$$

for $\Phi\to\epsilon\Phi_2+2\pi$.

To derive Eq. (2.14b) we must assume $r\Phi_2^2/(1-r)^2\ll 1$ for the validity of the expansion of Eq. (2.5). This condition requires Φ to be very small when $r\to 1$. Nonetheless this restriction is quite natural since the potential well is extremely narrow in this limit.

We now look for solutions of Eqs. (2.14a) and (2.14b) of the form

$$\phi_l(x,t)=\Psi_l(X,T)e^{-i\omega_l t}+\text{c.c.},\quad l=1 \text{ or } 2 \tag{2.15}$$

where it is assumed[13] that the variations in $\Psi(X,T)$ occur on a time scale very slow compared to ω_l^{-1} and a space scale large compared to a natural length scale in the system, i.e., the period of $V(\phi,r)$. Accordingly we introduce $T=\epsilon^2 t, X=\epsilon x$.

Inserting Eq. (2.15) in Eqs. (2.14a) and (2.14b) and keeping terms to order ϵ^2 we get, respectively, the two NLS equations,

$$i\Psi_{1T}+\frac{C_0^2}{2\omega_1}\Psi_{1XX}+k_1|\Psi_1|^2\Psi_1=0, \tag{2.16a}$$

$$i\Psi_{2T}+\frac{C_0^2}{2\omega_2}\Psi_{2XX}+k_2|\Psi_2|^2\Psi_2=0, \tag{2.16b}$$

where

$$k_1=\frac{\omega_1(1+r^2-4r)}{4(1+r)^2},\quad k_2=\frac{\omega_2(1+r^2+4r)}{4(1-r)^2},\quad 0<r<1.$$

The quantities C_0^2, ω_1, and ω_2 being positive, it turns out that the solutions of Eqs. (2.16a) and (2.16b) depend, respectively, on the coefficients k_1 and k_2. Let us first discuss the case of Eq. (2.16b) which is simpler. Indeed k_2 is always positive and the solution is an envelope soliton of the form[14–16]

$$\Psi_2(X,T)=\frac{(2\omega_2)^{1/2}}{C_0}\left[\frac{v_{2e}^2-2v_{2e}v_{2c}}{2k_2}\right](\text{sech}\theta)e^{i\sigma} \tag{2.17}$$

with

$$\theta=\frac{\omega_2}{C_0^2}(v_{2e}^2-2v_{2e}v_{2c})^{1/2}(X-v_{2e}T), \tag{2.18a}$$

$$\sigma=\frac{\omega_2}{C_0^2}\left[X-\frac{2\omega_2}{C_0^2}v_{2c}T\right]^{1/2}, \tag{2.18b}$$

where v_{2e} and v_{2c} are the velocities of the envelope and carrier waves. The corresponding low-amplitude breather solution is simply obtained by inserting Eq. (2.17) in Eq. (2.15).

For Eq. (2.16a) we have two cases. First, for $0<r<0.26$ k_1 is always positive and we have an envelope solution $\Psi_1(X,T)$ [similar to that given by Eq. (2.17) with velocities v_{1e} and v_{1c}] and as in the previous case we can easily get the corresponding breather solution. Second, for $0.26<r<1$ k_1 is negative; in that case the solution of (2.16a) is a "dark" (or a hole) soliton[17] which does not correspond to the small-amplitude limit of a breather mode. In other words no breather mode solution is possible for $0.26<r<1$ for the type-II solitons.

2. DWDP model

To look for the possibility of breather mode solutions we must consider the small nonlinear collective oscillations in the identical wells centered at $\phi=\pm\pi$. Thus introducing $\phi\rightarrow\epsilon\Phi_3+\pi$, Eqs. (2.5) and (2.2) yield

$$\Phi_{3tt}-C_0^2\Phi_{3xx}+\omega_3^2\left[\Phi_3-\frac{\epsilon^2\Phi_3^3}{6}+\frac{3\epsilon r}{1+r^2}\Phi_3^2\right]=0\ . \quad (2.19)$$

In contrast to the two previous cases we notice the presence of a Φ_3^2 term which is due to the asymmetry of each potential well [see Fig. 1(b)]. Consequently we must look[18] for asymmetric solutions which must contain at least a second harmonic term and also a constant term

$$\Phi_3(x,t)=\Psi_3^{(1)}(X,T)e^{-i\omega_3 t}+\text{c.c.}$$
$$+\epsilon[\Psi_3^{(0)}(X,T)+\Psi_3^{(2)}(X,T)e^{-2i\omega_3 t}+\text{c.c.}]\ . \quad (2.20)$$

With the same assumptions ($T=\epsilon^2 t$ and $X=\epsilon x$) as in the two previous cases Eq. (2.19) then becomes

$$\Phi_{3tt}-C_0^2\Phi_{3xx}+\omega_3^2\left[\Phi_3-\epsilon^2\frac{\Phi_3^3}{6}+\frac{3\epsilon r}{1+r^2}\Phi_3^2\right]-C_0^2\epsilon^2\Phi_{3XX}+2\epsilon^2\Phi_{3tT}+2\epsilon\Phi_{3xX}+O(\epsilon^4)=0\ . \quad (2.21)$$

Inserting Eq. (2.20) in (2.21) and equating dc, first harmonic, and second harmonic terms, we get, respectively,

$$\epsilon\left[\Psi_3^{(0)}+\frac{6r}{1+r^2}|\Psi_3^{(1)}|^2\right]+O(\epsilon^2)=0\ , \quad (2.22)$$

$$\epsilon^2\left[\frac{6r}{1+r^2}\omega_3^2(\Psi_3^{(1)}\Psi_3^{(0)}+\Psi_3^{(1)*}\Psi_3^{(2)})-\frac{\omega_3^2}{2}|\Psi_3^{(1)}|^2\Psi_3^{(1)}\right.$$
$$\left.-C_0^2\Psi_{3XX}^{(1)}-2i\omega_3\Psi_{3T}^{(1)}\right]+O(\epsilon^3)=0\ , \quad (2.23)$$

$$\epsilon\omega_3^2\left[-3\Psi_3^{(2)}+\frac{3r}{1+r^2}\Psi_3^{(1)2}\right]+O(\epsilon^2)=0\ . \quad (2.24)$$

With the help of Eqs. (2.22) and (2.24), we finally obtain from Eq. (2.23) the following NLS equation for $\Psi_3^{(1)}$:

$$i\Psi_{3T}^{(1)}+\frac{C_0^2\Psi_{3xx}^{(1)}}{2\omega_3}+k_3|\Psi_3^{(1)}|^2\Psi_3^{(1)}=0\ , \quad (2.25)$$

where

$$k_3=\omega_3\left[\frac{15r^2}{(1+r)^2}+\frac{1}{4}\right]\ .$$

The coefficient k_3 of this NLS equation is always positive for $0<r<1$ so that the envelope solution of Eq. (2.25) has a form similar to the solutions explicitly obtained in the previous cases [see Eq. (2.17)]. Knowing $\Psi_3^{(1)}$ one can calculate $\Psi_3^{(0)}$ and $\Psi_3^{(2)}$ from Eqs. (2.22) and (2.24) in terms of $\Psi_3^{(1)}$ and then easily deduce the corresponding small-amplitude breather solution from Eq. (2.20). For the sake of simplicity this complete solution will not be given here. The most important result is simply that for the DWDP model breather solutions exist for any value of the parameter r. For the ASDP and DWDP models the above theoretical results related to the existence of breather modes are confirmed by the results of our numerical simulations (see Sec. III).

III. PROPERTIES OF THE KINKS IN THE PERIODIC DOUBLE-WELL AND ASYMMETRIC POTENTIAL MODELS

In Sec. II we have shown that soliton solutions can be derived for the two models. The aim of this section is to present the properties of these solutions. For physical applications the stability of the excitations is especially important since long-lived excitations are expected (for instance) to play an important role in the thermodynamics of the system. Since it is well known that topological kinks are stable with respect to collisions with small (linear) excitations,[6] we have focused our attention on kink-kink interactions. Most of the results are obtained from numerical simulation and we first discuss briefly the numerical technique in Sec. III A. Then we examine the properties of the kinks in the two particular models that we have considered in Sec. I: the periodic double-well potential (Sec. III B) and the asymmetric periodic potential (Sec. III C). We show that interesting features are present in the two cases, some of them being useful to sharpen our understanding of kink interactions in other systems.

A. Numerical method

The numerical method used to simulate kink propagation in such models has been previously described.[6] Basically it consists in solving with a fourth-order Runge-Kutta method the Newtonian equations of motion of a discrete chain whose continuum analog is described by Eq. (2.5). This method has been specially designed to enable us to study the influence of the discreteness of the lattice which occurs naturally in many physical applications. In a previous study[6] the discreteness effects have been observed to be very sensitive to the exact shape of the potential. Indeed this is also true for the two models that we consider here. The case of the periodic double well is particularly interesting since two different discretization scales are simultaneously present in the system owing to the existence of two heights for the potential barriers. Nevertheless, a study of discreteness effects in the two models needs further investigations and they have been removed from the results that we present in the following by an appropriate choice of the kink width (typically 20 unit cells or more). The total number of unit cells in the system is either 400 or 600 with fixed boundaries. The time step Δt is chosen so that the total energy of the system is preserved to an accuracy better than 10^{-3} (typically $\Delta t=0.1$).

B. Properties of the kinks in the DWDP model

As previously mentioned, we are specially interested in the properties of the kinks (K) or antikinks ($\bar{K}$) when they

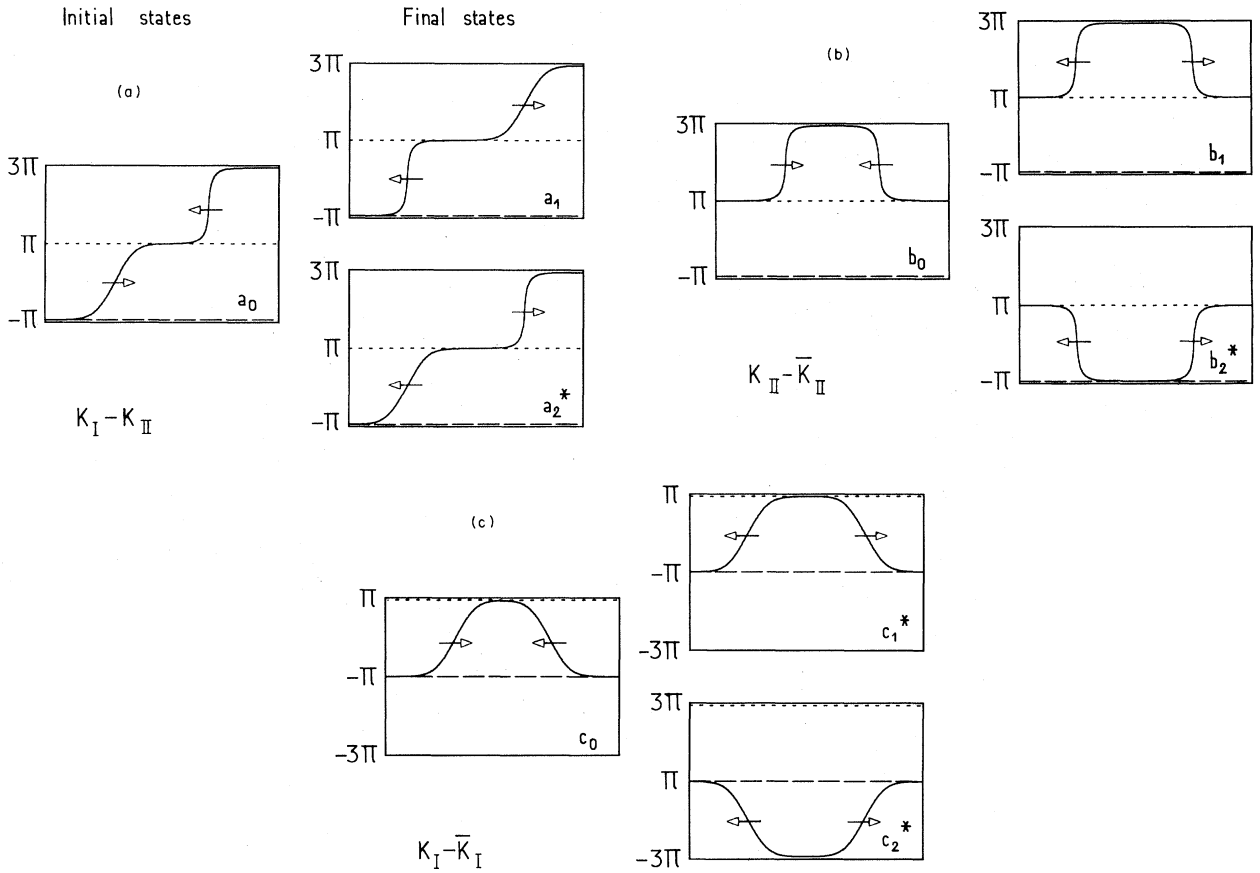

FIG. 3. Summary of the topological constraints governing kink collisions in the double-well potential. $(a_0),(b_0),(c_0)$ are the three possible initial states and $(a_1),(a_2),\ldots,$ the corresponding final states. The final states which are observed in the computer simulations are denoted by a star. Note that this picture is only schematic. For clarity the shapes of the kinks have been assumed not to vary in a collision. This is not true if a kink of a definite type (say type I) enters a domain of ϕ in which the other type is stable (for instance in C_2).

collide in order to determine their stability in a physical system which is expected to bear many of them (so that collisions necessarily occur). Results of Sec. II show that two types of kinks exist in the system. Type-I kinks with ϕ varying between $-\pi$ and $+\pi$ are associated with the lower barrier in the potential while the higher barrier corresponds to type-II kinks for which ϕ varies between π and 3π [Fig. 1(b)]. Kink masses M_{K_1} and M_{K_2} are such that $M_{K_1} < M_{K_2}$ (they are equal in the limit $r=0$, the SG case). Allowing for the existence of kinks (K) and antikinks ($\bar{K}$) of each type, one can imagine various kinds of collisions between these nonlinear excitations. Nevertheless, some of them are forbidden by the topological constraints in the system. Figure 3 shows that only three types of collisions have to be considered: K^{I}-K^{II} (or $\bar{K}^{\mathrm{I}}$-$\bar{K}^{\mathrm{II}}$ which is equivalent), K^{II}-$\bar{K}^{\mathrm{II}}$ and K^{I}-$\bar{K}^{\mathrm{I}}$. For a given initial state several final states are allowed by the topological constraints. They are plotted in Fig. 3. Similar properties occur in all systems with a doubly periodic substrate potential[10] and in particular in the double SG system.[19,20] In this last system only the second and third types of collisions ($K\bar{K}$ pair collisions) have been investigated for a particular shape of the potential.[19] We show in the following that, for these types of collisions, our results exhibit qualitative similarities with those obtained in the double SG model but rather large quantitative differences. Among these differences is the fact that the amplitude of the kinks $[\phi(+\infty)-\phi(-\infty)]$ remains constant (equal to 2π) in our model while, in the double SG system, the amplitude of the kinks corresponding to the lower barrier (type-I kinks) goes to zero as this barrier goes to zero, i.e., type-I kinks vanish.

1. K^{I}-K^{II} collisions

In these kink-kink collisions we observed that the final state is independent of the initial energy of the two excitations. The two kinks experience a repulsive interaction. Two processes for the collision are allowed by the topological constraints (Fig. 3): The two kinks can pass through each other or be reflected. In the SG case, for two indistinguishable initial excitations (two kinks with the same initial velocity) such a difference has no physical meaning (apart from the definition of the phase shift in the collision) but this is not the case here when the parameter r is different from zero: Even two kinks with the same initial velocity have different masses and shapes (and particularly different widths). Let us consider what would happen if the two kinks pass through each other. A type-II kink

would enter the domain $-\pi<\phi<+\pi$ (which is the domain of stability of a type-I kink) while a type-I kink would enter the domain $\pi<\phi<3\pi$. Thus the two excitations would have to adjust their shapes to recover the shape which corresponds to the solution in the region which they have entered. The deformation energy required for the adjustment would be subtracted from the kinetic energy of the kinks. Although such a mechanism is topologically allowed (and occurs in the case of asymmetric kinks as we shall see in the next section) a careful examination of the state of the system during the collisions shows that the two kinks reflect each other when they collide, each of them staying in the domain where it is stable (final state a_2 in Fig. 3). As a consequence the energy of the kinks is preserved nearly perfectly in the collision. If the kinks are considered as relativistic pseudoparticles[3] with masses M_{K_1} and M_{K_2} and velocities $v_{\rm I}$ and $v_{\rm II}$ before the collision and $v'_{\rm I}, v'_{\rm II}$ after the collision, energy and momentum conservation yield

$$\frac{M_{K_1}}{(1-v_{\rm I}^2/C_0^2)^{1/2}}+\frac{M_{K_2}}{(1-v_{\rm II}^2/C_0^2)^{1/2}} =\frac{M_{K_1}}{(1-v_{\rm I}'^2/C_0^2)^{1/2}}+\frac{M_{K_2}}{(1-v_{\rm II}'^2/C_0^2)^{1/2}}\ , \tag{3.1a}$$

$$\frac{M_{K_1}v_{\rm I}}{(1-v_{\rm I}^2/C_0^2)^{1/2}}+\frac{M_{K_2}v_{\rm II}}{(1-v_{\rm I}^2/C_0^2)^{1/2}} =\frac{M_{K_1}v'_{\rm I}}{(1-v_{\rm I}'^2/C_0^2)^{1/2}}+\frac{M_{K_2}v'_{\rm II}}{(1-v_{\rm II}'^2/C_0^2)^{1/2}}\ . \tag{3.1b}$$

Relations (3.1a) and (3.1b) have been checked in different cases ($r=0.1$ and 0.3) with initial velocities between $0.1C_0$ and $0.5C_0$. They are verified to an accuracy of 0.3—5 % which lies inside the accuracy of our numerical experiment (this accuracy is better for the higher velocity cases). However, a careful examination of the kink shapes after their collision shows slight modifications which indicate that a small part of the energy of the incident kinks has been transferred into deformation energy of the kinks. But this loss of energy is so small that we cannot "measure" it in the numerical experiment. Thus, as far as only kink-kink collisions are concerned, the picture of the kinks as forming an ideal gas made of two types of relativistic particles appears to give an accurate description of the properties of the system. Nevertheless, the two following sections show that when antikinks are present the picture is not so simple since conversions of particles of type II into type I (or vice versa) can occur.

2. $K^{\rm II}$-$\bar{K}^{\rm II}$ *collisions*

As in the previous case, in such a collision two states are allowed by the topological constraints. If the two excitations repel each other the final state is again a $K^{\rm II}$-$\bar{K}^{\rm II}$ pair (final state b_1 in Fig. 3) but if they pass through each other they are converted into a $K^{\rm I}$-$\bar{K}^{\rm I}$ pair (final state b_2 in Fig. 3). The relation $M_{K_1}>M_{K_2}$ shows that the $K^{\rm II}$-$\bar{K}^{\rm II}$ pair has always sufficient energy (whatever the initial velocities of the excitations) to form a $K^{\rm I}$-$\bar{K}^{\rm I}$ pair. We observe that this conversion into type I always occurs. As a result in a $K^{\rm II}$-$\bar{K}^{\rm II}$ collision, the two excitations never form bound state (breather mode). It is interesting to note that the picture of relativistic quasiparticles for the kinks is again valid here if one allows for a possible conversion of the heavy type-II particles into light type-I particles. The difference between the rest energies is converted into kinetic energy of the light particles according to the energy conservation relation:

$$\frac{2M_{K_2}}{(1-v_{\rm II}/C_0^2)^{1/2}}=\frac{2M_{K_1}}{(1-v_{\rm I}^2/C_0^2)^{1/2}}\ . \tag{3.2}$$

Computer simulations show that this energy conservation is verified with a rather good approximation: Let us illustrate this assertion by a numerical result. In the case $r=0.3$ the ratio of the rest masses of the particles is $M_{K_2}/M_{K_1}=2.6024$. When two heavy (type-II) particles collide with initial velocities $\pm 0.1C_0$ we observe the formation of a pair of light particles (type I) with velocities $\pm 0.90C_0$ while the energy conservation would yield $0.924C_0$. In such a collision a slight decrease in the energy of the quasiparticles was expected because when the type-II kinks pass through each other they enter the domain in which the type-I kinks are stable ($-\pi<\phi<+\pi$) and thus they have an inappropriate shape. The adjustment of their shape toward that of type-I kinks is accompanied by the emission of small-amplitude excitations which carry away a part of the energy of the quasiparticles. Nevertheless, the numerical results show that this radiation has a rather weak effect on the energy of the kinks and this is even more exact if their initial velocities are higher. In a $K^{\rm II}$-$\bar{K}^{\rm II}$ collision, the topological constraints do not exclude a third final state in which four excitations would be produced, i.e., a $K^{\rm I}$-$\bar{K}^{\rm I}$ pair plus a $K^{\rm II}$-$\bar{K}^{\rm II}$ pair moving slowly, as shown in Fig. 4. If the kinetic energy of the initial $K^{\rm II}$-$\bar{K}^{\rm II}$ pair is sufficient, this final state may also be consistent with energy conservation in the system. However, as in the double SG model,[19] numerical simulations never show this double pair production:[21] The number of quasiparticles is always conserved in a collision.

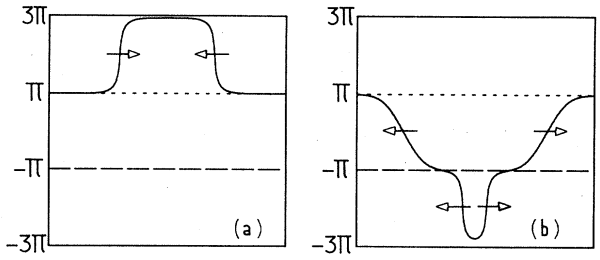

FIG. 4. Schematic picture showing that the production of two pairs of kinks from a $K^{\rm II}$-$\bar{K}^{\rm II}$ collision in the DWDP model is allowed by the topological constraints: (a) initial state, (b) final state. This double pair production is not observed in the numerical simulations.

3. K^{I}-$\bar{K}^{I}$ collisions

Simulations of K^{II}-$\bar{K}^{II}$ collisions have indicated that the quasiparticle picture is again rather accurate provided that the possibility of the conversion between the two types of particles is introduced in the model. The study of K^{I}-$\bar{K}^{I}$ collisions confirms this result. This type of collision involves solitons which correspond to the small barrier of the periodic double well and consequently it exhibits some similarities with a K-$\bar{K}$ collision in the ϕ^4 model. But a major difference exists: In our case the barrier between two double wells is finite. Whereas in the ϕ^4 case kink and antikink can never pass through each other, in the periodic double well this topological constraint is removed. Nevertheless, one must also take into account energetic constraints. As shown schematically in Fig. 3 (final state C_2) when K^{I} and $\bar{K}^{I}$ pass through each other they form a K^{II}-$\bar{K}^{II}$ pair. As a consequence their initial energy must be at least equal to twice the rest mass M_{K_2} of the type-II kinks. Since $M_{K_1} < M_{K_2}$ this can be achieved only if the K^{I}-$\bar{K}^{I}$ pair has enough kinetic energy, i.e., if the initial velocity v_i of the two excitation exceeds a value v_i^0 given by

$$\frac{2M_{K_1}}{[1-(v_i^0)^2/C_0^2]^{1/2}} = 2M_{K_2} . \tag{3.3}$$

For instance, for $r=0.3$ this equation gives $v_i^0 = 0.784 C_0$. In fact this value is only a lower limit since the K^{II}-$\bar{K}^{II}$ pair generated with no kinetic energy is not stable: The two excitations experience an attractive interaction which brings them together and this collision again creates a K^{I}-$\bar{K}^{I}$ pair. The conversion of light kinks into heavy ones is only observed for input velocities greater than $0.92 C_0$. When $v_i < v_i^0$ the two kinks can never pass through each other and for this velocity range the model becomes equivalent to a model with infinite double wells. In this case the final state is still sensitive to the initial velocity of the two colliding excitations ($v_i < v_j^0$). There is a critical velocity v_c such that the two kinks can reflect from each other and escape to infinity only if $v_i > v_c$. Two points have to be discussed: the variation of the critical velocity as a function of the shape parameter r and the behavior of the two excitations for $v_i < v_c$. Let us consider successively these two points.

When a kink and an antikink collide they interact through an attractive potential.[22–24] If the energy of the excitations is exactly preserved during the collision, K and $\bar{K}$ can always escape from this attractive well, even if their initial kinetic energy is very low or equal to zero. This is the case in an integrable model like the SG model and the critical velocity is zero in such a model. But if the K and $\bar{K}$ lose some energy in the collision process they may be trapped by their attracting potential and form a bound state.[24,8] This trapping occurs if their initial kinetic energy is smaller than the energy that they lose in the collision. This condition determines the critical velocity v_c. Consequently the value of the critical velocity gives an indirect measure of the loss of energy in a K-$\bar{K}$ collision and particularly $v_c \neq 0$ means that the kinks are not strict solitons (i.e., that the model is not completely integrable). The critical velocity in a K^{I}-$\bar{K}^{I}$ collision is plotted in Fig. 5 as a function of r. In the whole domain $0.03 < r < 1$ the variation of v_c is confined in the small range $0.06 < v_c < 0.16$. The rather sharp increase of v_c for $r < 0.03$ is not a surprise since this domain corresponds to the transition from a completely integrable model (SG model) to a nonintegrable one.[6,9] More remarkable, and up to now unexplained, is the minimum of v_c which is observed for $r=0.3$. For this value of r the shape of the potential is far from a sinusoidal shape (for instance the ratio of the large and small barrier heights is 0.084) but the K-$\bar{K}$ collisions are nearly elastic, i.e., the kinks in this model behave as "nearly exact solitons." This is clear in Fig. 6 where the output velocities of the two excitations are plotted versus their input velocities for the DWDP model with $r=0.3$ and other models (SG, ϕ^4, or double SG models): The curve for the DWDP model is very close to that of the SG

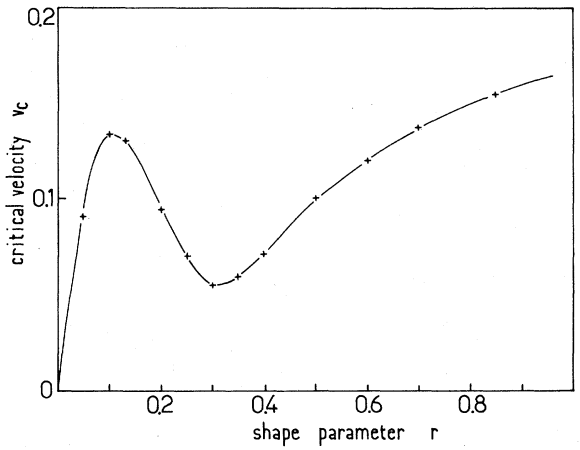

FIG. 5. Critical velocity for K^{I}-$\bar{K}^{I}$ collisions in the DWDP model as a function of the shape parameter r.

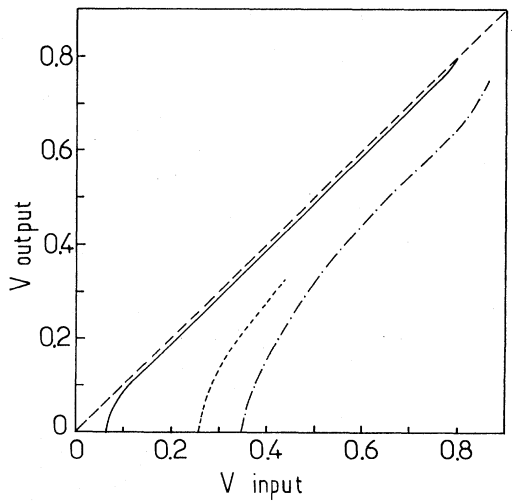

FIG. 6. K-$\bar{K}$ outgoing velocities as a function of their incoming velocities for a K^{I}-$\bar{K}^{I}$ collision in the DWDP model for $r=0.3$ (solid line) compared with the same results for the SG model (dashed line), ϕ^4 model (dotted line) (from Ref. 24), and double SG model (dotted-dashed line) (from Ref. 19).

model. This result shows that the picture of kinks as quasiparticles performing nearly elastic collisions ceases to be valid only in a very small domain of initial velocities ($v_i < v_c$).

As previously mentioned for $v_i < v_c$, the colliding kink and antikink are trapped in their attracting potential. In agreement with the theoretical results of Sec. II, we observe that they form an oscillating bound state (breather mode) for all values of the shape parameter r. Figure 7 represents the position of the center of the chain $\phi(x=0,t)$ as a function of time for a K^{I}-$\bar{K}^{\mathrm{I}}$ collision at low initial velocity. This figure shows clearly the existence of a rather stable oscillating state. It is important to notice that $\phi(0,t)$ is not symmetric with respect to the bottom of the potential well (contrary to the SG breather, for instance). This is related to the asymmetry of each well in the DWDP model.

In the theoretical derivation of the small-amplitude breather solution (Sec. II) this asymmetry was taken into account by the introduction of a second harmonic ($e^{2i\omega t}$ term) which is responsible of the particular shape of the function $\phi(0,t)$. In addition, Fig. 7 clearly shows the existence of the dc term which was introduced in the theoretical treatment to derive the breather solution. Thus the theory proposed in Sec. II proves very efficient in spite of the approximation of small-amplitude breather modes which is made.

C. Properties of the kinks in the ASDP model

Similarly to the DWDP model, this model also bears two types of kinks. Type-I kinks ($0 < \phi < 2\pi$) and type-II kinks ($2\pi < \phi < 4\pi$) have now the same rest masses M_{K_1} and M_{K_2}. We can again consider the same kind of collision as for the DWDP model (see Fig. 3): K^{I}-K^{II}, K^{II}-$\bar{K}^{\mathrm{II}}$, and K^{I}-$\bar{K}^{\mathrm{I}}$. As shown in Sec. II, each kink is asymmetric, due to the asymmetry of the potential barrier and this is responsible of an interesting new property of this model. As previously mentioned an ASDP kink separates two "media" which are physically inequivalent. Thus the introduction of a kink in a chain creates a symmetry

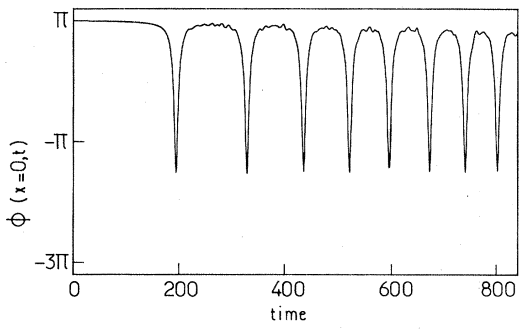

FIG. 7. Position of the center of the chain $\phi(x=0,t)$ as a function of time in a K^{I}-$\bar{K}^{\mathrm{I}}$ collision in the DWDP model for an initial velocity smaller than the critical velocity ($r=0.3, v_i=0.04$) showing the formation of a rather stable breather mode. Note the asymmetry and dc shift of the breather oscillation with respect to the bottom of the well ($\phi=-\pi$).

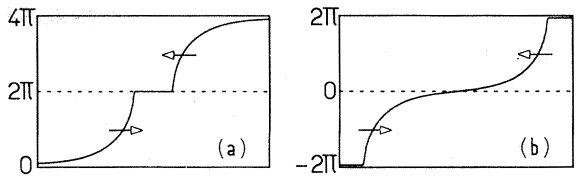

FIG. 8. The two types of kink-kink collisions in the ASDP model: (a) hard collision, (b) soft collision.

breaking and introduces an orientation of the medium: the two directions $+x$ and $-x$ are no longer equivalent. But the kink itself is orientated. Its shape is different in the two directions $+x$ and $-x$ and so are its interactions with other kinks in the system. This property dominates the kink interactions in the ASDP model.

1. K^{I}-K^{II} collisions

Contrary to the previous case we have now to consider two types of kink-kink collisions in the system as shown in Fig. 8. In the first case the two kinks move toward each other with their sharp edge in front of them. They ignore each other until they are very close to each other and then collide abruptly. We call such a collision a "hard collision." On the contrary, in the second case the two kinks present each other their smooth edge and thus experience a repulsive interaction even when they are far from each other. Such a collision is henceforth called a "soft collision." As one would expect the results of the two collisions are totally different.

Hard collisions are highly inelastic because, except for very low input velocities, the two kinks pass through each other. This is checked by the observation of the system immediately after the collision (Fig. 9 shows an example

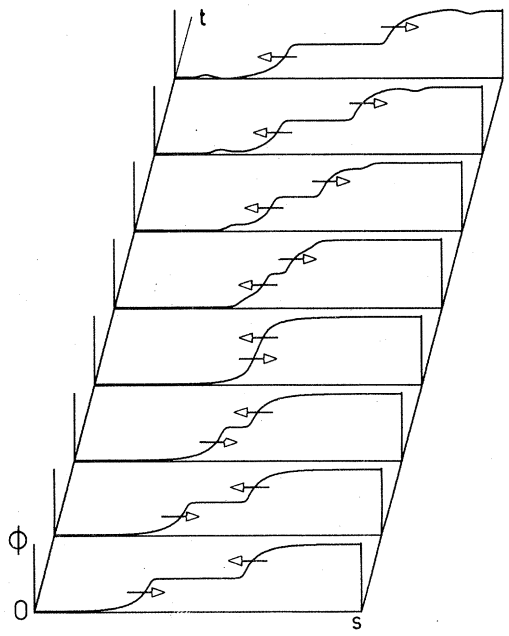

FIG. 9. K^{I}-K^{II} collision (hard collision) in the ASDP model.

of such a collision). As pointed out previously if such a situation occurs in a system bearing two different types of kinks, after their collision, the kinks enter domains in which their shape does not correspond to the solution of the equation of motion. Figure 9 shows the remarkable stability of the kink solutions in such systems carrying topological kinks: The two excitations quickly adjust their shape to recover the shape which is stable in the domain they have just entered. This shape modification is accompanied by the emission of a small bump (which propagates at speed C_0 almost without deformation along the chain as shown in Fig. 9). This bump indeed carries some energy which is subtracted from the kinetic energy of the kinks after the collision. This is indicated by a drop in the kink velocities which becomes more and more pronounced as the incoming velocities of the kinks increase because the collision gets more and more violent, as shown in Fig. 10 where the output velocities of the kinks are plotted versus their initial velocities in the case $r=0.5$.

On the contrary in a soft collision the kink and antikink experience a repulsive interaction which increases smoothly. They reflect from each other without any modification of their shape and their collision is almost perfectly elastic within the accuracy of the numerical experiment: Their velocity is conserved to an accuracy of $0.001C_0$ up to initial velocities equal to $0.8C_0$ and even when their input velocity is $0.9C_0$ the decrease in output velocity is less than $0.005C_0$, as shown in Fig. 10.

2. *Kink-antikink collisions*

The orientated character of the interaction between two kinks is also present in kink-antikink interactions. Figure 11 shows the two types of K-$\bar{K}$ collisions which are topologically permitted in the model. The K^{I}-$\bar{K}^{\mathrm{I}}$ collision is a hard collision while the K^{II}-$\bar{K}^{\mathrm{II}}$ collision is a soft collision. Consequently the critical velocities $v_{c\mathrm{I}}$ and $v_{c\mathrm{II}}$

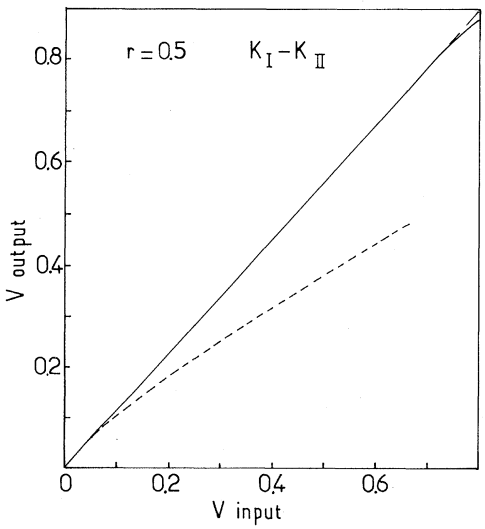

FIG. 10. Outgoing velocities of the kinks as a function of their incoming velocities for the two types of K^{I}-K^{II} collisions in the ASDP model: soft collision (solid line) and hard collision (dashed line).

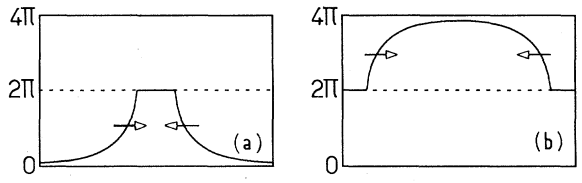

FIG. 11. Two types of kink-antikink collisions in the ASDP model: (a) K^{I}-$\bar{K}^{\mathrm{I}}$ (hard collision), (b) K^{II}-$\bar{K}^{\mathrm{II}}$ (soft collision).

under which the two excitations are unable to escape from their attracting interaction potential are expected to be significantly different.

This is indeed the case as shown in Fig. 12, where $v_{c\mathrm{I}}$ and $v_{c\mathrm{II}}$ are plotted as a function of r. In both cases, when their initial velocities v_i are such that $v_i > v_c$, the two excitations pass through each other and escape to infinity. As explained previously the loss of energy in this process is important and both $v_{c\mathrm{I}}$ and $v_{c\mathrm{II}}$ are high. Nevertheless Fig. 12 shows that $v_{c\mathrm{I}}$ (corresponding to the hard collision) is much greater than $v_{c\mathrm{II}}$ (corresponding to the soft collision) as expected. When r is greater than 0.5, even excitations with $v_i = 0.95C_0$ cannot escape to infinity. Since $v_{c\mathrm{I}}$ and $v_{c\mathrm{II}}$ are very high it is of particular importance here to study the behavior of the two excitations when they collide at velocities which are smaller than the critical velocities. In these cases the K-$\bar{K}$ interactions exhibit a rich phenomenology. In Sec. II we have shown that breather modes exist for all values of r in the narrow potential well ($\phi \sim 2\pi$) while they only exist in the large potential well ($\phi \sim 0$) if $r < 0.26$. This result is exactly confirmed by the numerical simulations. The case $\phi \sim 2\pi$ corresponds to K^{II}-$\bar{K}^{\mathrm{II}}$ collisions and we have actually been able to generate rather stable breather modes in this

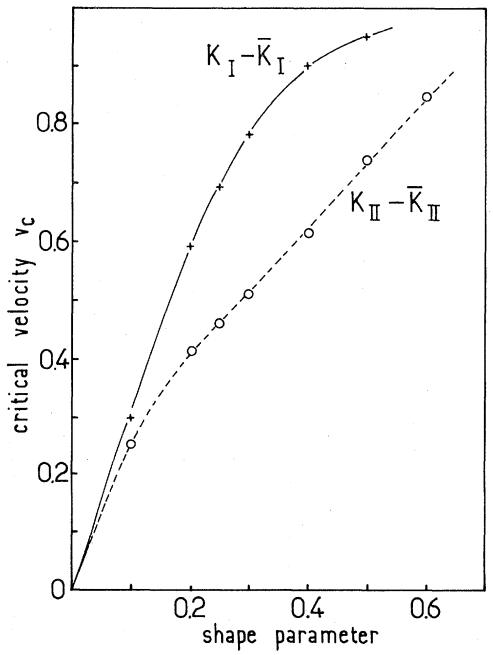

FIG. 12. Critical velocites $v_{c\mathrm{I}}$ and $v_{c\mathrm{II}}$ in the ASDP model as a function of the shape parameter r.

case for various values of r but, as we will discuss later, these solutions are not obtained for all values of $v_i < v_{CII}$. K^{I}-$\bar{K}^{I}$ collisions correspond to the case $\phi \sim 0$. When r is small ($r < 0.15$) we observe large-amplitude, rather stable breathers but when r increases over 0.15 the amplitude of the breather mode which stays in the middle of the chain decreases while more and more energy is transfered into two bumps which are formed in the hard K-$\bar{K}$ collision. This effect is shown in Fig. 13. We have been unable to generate any stable breather in a K^{I}-$\bar{K}^{I}$ collision for $r > 0.3$ Thus the limit $r = 0.26$ does not appear as a sharp limit in the numerical simulation. It is nonetheless remarkable that a theory assuming only low-amplitude solutions gives a good estimate of the existence of the breathers produced in a K-$\bar{K}$ collision which generates large-amplitude breathers.[25]

K^{II}-$\bar{K}^{II}$ collisions are not only interesting because they can create breather modes but also because *resonant K-$\bar{K}$ interactions* exist in this case. As pointed out previously for most of the initial velocities $|v_i| < v_{CII}$ the K^{II} and $\bar{K}^{II}$ form an oscillatory decaying bound state. But in well-defined "windows" of $|v_i|$ below v_{CII} the K^{II}-$\bar{K}^{II}$ pass through each other once, escape to finite distance, and then return to pass through each other once more before separating to infinity. This particular behavior has been studied in detail for the case $r = 0.1$ and is only possible when r is not too high ($r < 0.4$). This type of resonant interaction was first observed in the ϕ^4 model[24–28] and very recently an explanation of these "two-bounce windows" in terms of a resonant energy exchange between the translational motion of the K and $\bar{K}$ and a localized internal oscillation has been proposed.[24] Similar resonances were also discovered[8] in the model derived from Eq. (1.1) and previously studied.[5,6] In this case the possibility to change the shape of the potential by varying r (and then to modify the number of internal modes of the kinks) was used to test more precisely the role of the internal modes in resonant interactions. Since the previous study was rather complete (and involved a tremendous amount of numerical calculation) it is not our aim here to perform a similar study on a new type of deformable potential but only to stress a few points that bring new features to the theory of these resonant interactions.

The outgoing velocity of the kinks as a function of their incoming velocity is plotted in Fig. 14. In addition to the existence of the critical velocity $v_{CII} = 0.251$, Fig. 14 shows the presence of six narrow windows for $v_i < v_{CII}$ in which the kink outgoing velocities are nonzero. (Note however that the widths of these windows are not their actual widths. They are extremely narrow—$\Delta v_i < 0.005$ for the larger one—and we did not attempt to determine their actual widths. Similarly, to save computation time we did not perform a systematic research of additional windows very close to v_{CII}, although there are strong indications in our results that at least two additional windows exist.)

A detailed theoretical interpretation of the resonance windows has been presented earlier[14,8] and we just outline here the main ideas of this interpretation. It involves a localized internal oscillation of the kink K^{II} (the "shape mode") which corresponds to a discrete eigenvalue ω_B of the Schrödinger-type equation that governs the small oscillations $\delta\phi(x,t) = f(x)e^{i\omega t}$ about the kink waveform:

$$-f_{xx} + \left[\frac{\omega_0^2}{C_0^2}\right]\mathscr{V}_{II}(x)f(x) = \left[\frac{\omega^2}{C_0^2}\right]f(x)\,, \tag{3.4}$$

where $\mathscr{V}_{II}(x)$ is obtained from the second derivative of the ASDP potential:

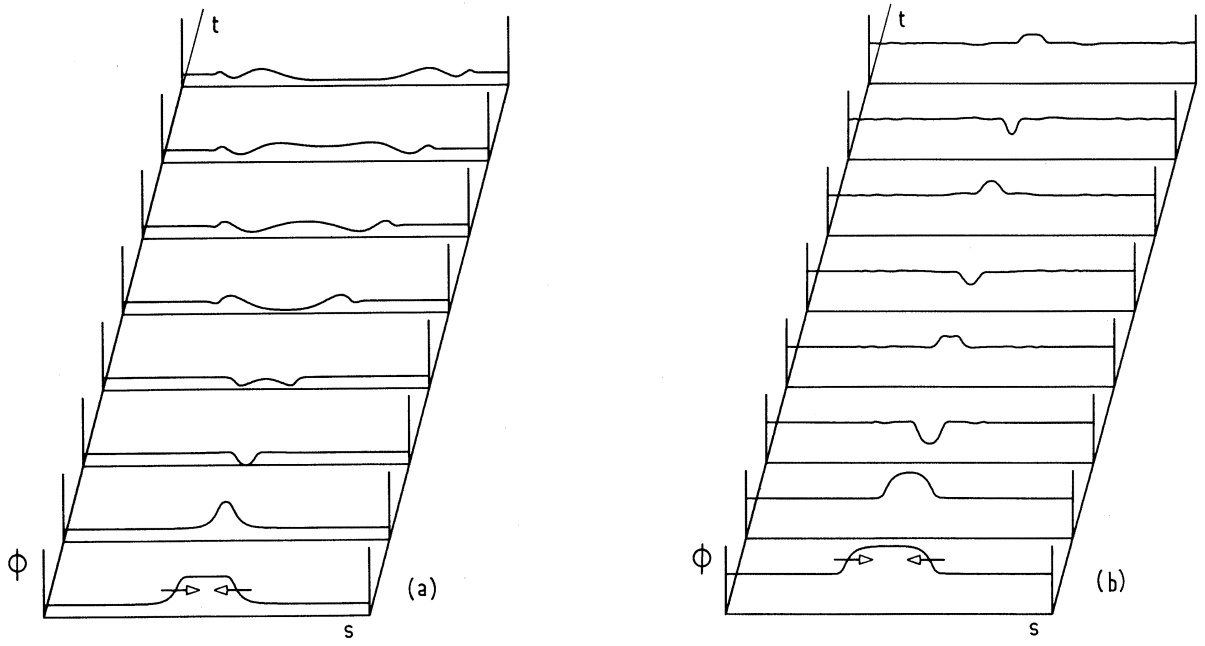

FIG. 13. (a) K^{I}-$\bar{K}^{I}$ and (b) K^{II}-$\bar{K}^{II}$ collisions in the ASDP model for $r = 0.3$ for kink incoming velocities smaller than the critical velocities v_{CI} and v_{CII}. Note that in this case ($r > 0.26$) only the K^{II}-$\bar{K}^{II}$ collision gives rise to a breather mode in agreement with the theoretical predictions.

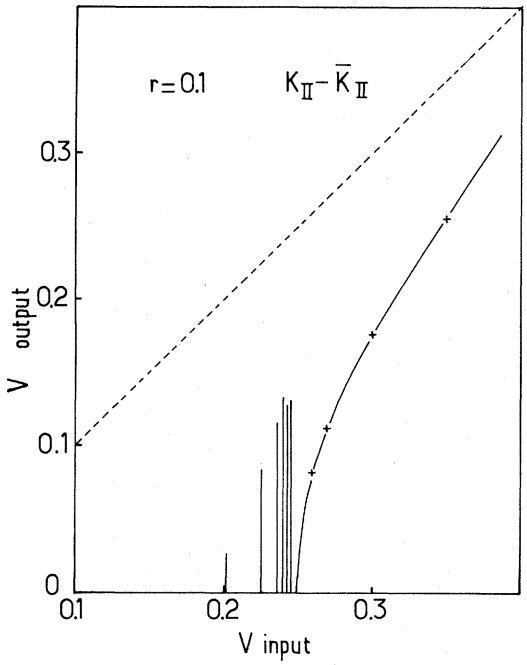

FIG. 14. K^{II}-$\bar{K}^{II}$ outgoing velocites as a function of their incoming velocities for $r=0.1$ in the ASDP model. The bars indicating resonances for $v_i < v_{CII}$ are only schematic since these resonances are very sharp. The dashed line would correspond to an integrable model ($v_{output}=v_{input}$).

$$\mathscr{V}_{II}(x)=\frac{d^2V}{d\phi^2}[\phi_{K^{II}}(x)] \ . \tag{3.5}$$

The potential $\mathscr{V}_{II}(x)$, obtained numerically, is plotted in Fig. 15 for various values of r. Note that the two limits of this potential for $x\rightarrow+\infty$ or $x\rightarrow-\infty$ are different. This is simply related to the fact that the two media on the two sides of the kink are inequivalent. The resonance condition is given by

$$\omega_B T_n = 2\pi n + \delta \ , \tag{3.6}$$

δ is a constant and T_n is the time which separates the two kink collisions before they escape to infinity for a given window characterized by the integer index n. T_n is the time during which the kink and antikink are bounded by their attractive interaction potential. With some simplifying assumptions T_n can be shown to be

$$T_n=\frac{\beta}{(v_{CII}^2-v_n^2)^{1/2}} \ , \tag{3.7}$$

β being a constant and v_n the initial velocity corresponding to the window of index n. Thus, using Eqs. (3.6) and (3.7), v_n is given by

$$v_{CII}^2-v_n^2=\frac{\beta^2\omega_B^2}{(2n\pi+\delta)^2} \ . \tag{3.8}$$

In spite of its simplifying assumptions, this theory proved very accurate to describe resonances in the ϕ^4 (Ref. 24) and deformable periodic potential[8] models and here again it gives a good estimate of the position v_n of the windows.

The dependence of T_n versus an integer index n is found to be exactly linear within the accuracy of our experiment [i.e., Eq. (3.6) is satisfied] as shown in Fig. 16. The slope of the line gives $\omega_B=0.9235$ and $\delta=-3.077$. This curve also determines n for each resonance. This value of n can, however, also be derived from the number of kink "internal" oscillations between the two kink collisions observed in the numerical experiment. The product $T_n(v_{CII}^2-v_n^2)^{1/2}$ varies between 3.51 and 3.10 with a mean value $\beta=3.306$. Thus Eq. (3.7) is satisfied to an accuracy of 12%. Table II compares the theoretical values of v_n and the values determined numerically. Table II shows that the theoretical interpretation of the resonant interactions is able to describe rather well the observed phenomena (note that all the parameters β,ω_B,δ are determined "experimentally" and thus no adjustable parameter is introduced in the model). The best agreement is obtained for the resonances corresponding to indexes 5 to 7 because, as shown previously, the value of β varies slightly with n and we have used the average value which is accurate for $n=6$. A theory taking into account this slight variation of β would indeed give even better results.

Contrary to the case of the K^{II}-$\bar{K}^{II}$ collision, in spite of a careful search we never found any resonant interaction

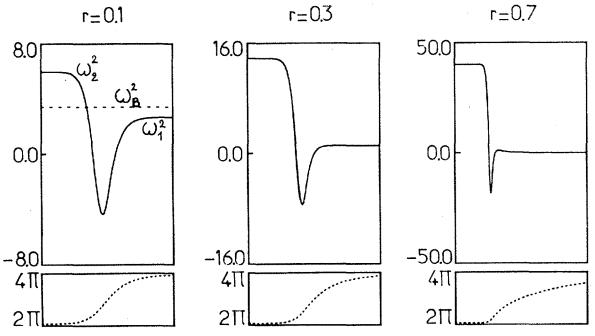

FIG. 15. Potential $\mathscr{V}_{II}(x)$ for the small-amplitude oscillations about the K^{II} waveform in the ASDP model for different values of r. Note the different scales when r increases. The kink profiles at the bottom give the scale in the x direction.

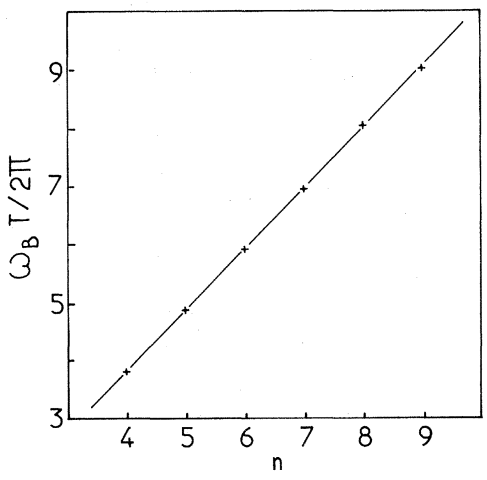

FIG. 16. $\omega_B T_n/2\pi$ as a function of the window index n for the resonances in K^{II}-$\bar{K}^{II}$ collisions in the ASDP model.

TABLE II. Two-bounce resonant windows in K^{II}-$\bar{K}^{II}$ scattering for the ASDP model ($r=-0.1$).

Index n	Center of the window v_n (numerical simulation)	Theoretical value of v_n
4	0.202	0.2094
5	0.224	0.2267
6	0.234	0.2355
7	0.240	0.2396
8	0.2434	0.2425
9	0.2452	0.2444

in a K^{I}-$\bar{K}^{I}$ collision. This result is not in agreement with the theory previously proposed to explain the resonances.[24,8] Owing to the shape of the two types of kinks [see Fig. 1(a)] we have the following relation between the two potentials $\mathscr{V}_{I}(x)$ and $\mathscr{V}_{II}(x)$ of the Schrödinger-type Eq. (3.4):

$$\mathscr{V}_{I}(x)=\mathscr{V}_{II}(-x) .$$

Moreover, Eq. (3.4) is invariant in the change of x into $-x$. As a result the spectrum of the small oscillations about the two types of kink is the same. According to the theory previously proposed[24,8] the existence of resonances is directly connected to the existence of discrete eigenvalues in this spectrum and thus the resonances should be present (or absent) in both cases. So this theory has to be modified for the new case of kinks separating two media (henceforth labeled medium 1 and medium 2) which have not the same phonon spectrum. The relative positions of the energy levels ω_1^2, ω_2^2, and ω_B^2 are indicated in Fig. 15 [showing $\mathscr{V}_{II}(x)$] in the case $r=0.1$; they are, respectively, 0.6694, 0.8529, and 1.4938 (in units of ω_0^2). It is clear from this figure that *the oscillatory state with energy ω_B^2 is not a localized state,* but a state bounded only in one direction: Oscillations at frequency ω_B can propagate in medium 1 which admits ω_1 as lowest phonon frequency (i.e., in the medium where $\phi\sim 0$ or 4π) and they cannot propagate in medium 2 which has ω_2 as lowest phonon frequency ($\phi\sim 2\pi$) due to the relation $\omega_1<\omega_B<\omega_2$. Once this remark has been made, the difference between the K^{I}-$\bar{K}^{I}$ and K^{II}-$\bar{K}^{II}$ collisions is easily understood by looking at Fig. 11 which shows the state of the system for these two collisions. In a K^{II}-$\bar{K}^{II}$ collision medium 1 is situated between the two kinks while in a K^{I}-$\bar{K}^{I}$ collision it is situated outside the domain limited by the two kinks. Consequently, although it is not localized near one kink, in the K^{II}-$\bar{K}^{II}$ collision, *the oscillation at frequency ω_B is confined between the two excitations;* the energy which is temporarily stored in this mode cannot escape to infinity; if the resonance condition is satisfied, this energy can be restored to the two kinks and a resonance occurs. On the contrary in a K^{I}-$\bar{K}^{I}$ collision the energy stored in the oscillatory mode is situated outside the domain separating the two kinks and escapes to infinity. Thus no resonance can exist.

The example of K-$\bar{K}$ collision in the ASDP model shows clearly the new features which emerge in this model where a kink interpolates between two different "media," i.e., with different characteristic phonon frequencies.

IV. CONCLUSION

Since each of the preceding sections has contained substantial discussion and analysis we simply summarize here the main conclusions. Among a large variety of models that can be obtained from the generalized potential that we have introduced we have focused our attention on two cases of doubly periodic potential since it is a natural way for generalizing to a lattice with diatomic basis those lattice dynamical models that assume simple singly periodic potentials.[10] These models [with double well deformable periodic potential (DWDP) or asymmetric deformable potential (ASDP)] bear two types of kinks and are continuously deformable in a controlled manner from the sine-Gordon model.

The DWDP model has some common features with the double SG model, which has recently attracted some attention for its statistical mechanics properties,[10,29] in the sense that it contains two kinks with different masses. The main characteristic feature of this model, although it is not completely integrable, is that kink properties are very close to those of a completely integrable system and in particular the initial velocity below which K and $\bar{K}$ cannot escape from their attractive potential is very low (and exhibits a minimum for a particular shape of the potential). Thus kink properties are well described by treating the excitations as relativistic quasiparticles of two different types (type I with mass M_{K_1} and type II with mass M_{K_2}) if conversion between the two types of articles is possible with particle number conservation and their interactions verify nearly exactly the conservation of relativistic energy and momentum.

We believe that the introduction of the ASDP model brings may interesting new features for physical applications. Not only are kinks asymmetric in this model but they interpolate between two "media" with different physical properties (especially phonon frequencies). These two media could be for instance two different crystallographic phases coexisting at a first-order phase transition (and not only two domains of the same phase with different polarizations as in a double-well model). This property poses challenging new problems for the statistical mechanics of the system since the motion of the kinks changes the properties of the medium in which they move. Among the new properties of this model is the possibility of confinement of phonon oscillations between the two kinks forming one of the two topologically allowed K-$\bar{K}$ pairs, which is responsible of resonant interactions between the two kinks.

The asymmetry of the kinks also influences their interaction with other kinks. In a particlelike picture kinks correspond to particles that interact with a short-range interaction on one side (the side of the sharp edge of the kink) and with a long-range interaction on the other side (the side of the smooth edge of the kink).

Another area of interest emerges from the difference between the DWDP kinks and ASDP kinks which is well illustrated if one considers an array of kinks (as those

which are used to model incommensurate crystals[30]). On one hand (DWDP model), one would get a diatomic lattice of particles with masses M_{K_1} and M_{K_2} alternating regularly due to the topological constraints and experiencing identical interactions. On the other hand (ASDP model), we obtain a lattice of particles carrying an internal orientation (that we could modelize by a pseudospin) with identical masses; these particles have alternating orientations which are responsible for two different alternating interaction forces between them. As a result from a mechanical point of view the two kinds of lattices are dual lattices.

Moreover, looking for breather solutions as the low-amplitude limit of nonlinear Schrödinger envelope solitons, we have analytically determined necessary conditions for the existence of breather modes. The results are remarkably confirmed by the numerical experiments even for the large-amplitude breathers created by kink-antikink collisions. It suggests that the theoretical approach employed is quite general.

We hope that these two models together with the large family of deformable potentials that we have introduced in this paper will prove useful in modeling a rich variety of physical systems.

ACKNOWLEDGMENT

We wish to thank D. Campbell (Center for Nonlinear Studies, Los Alamos National Laboratory) for enjoyable and fruitful discussions held during his visit in Laboratoire ORC.

---

*Present address.

[1]See, for example, *Solitons in Action,* edited by K. Lonngreen and A. C. Scott (Academic, New York, 1978), and also *Solitons in Condensed Matter Physics,* edited by A. R. Bishop and T. Schneider (Springer, New York, 1978).

[2]J. Frenkel and T. Kontorova, J. Phys. (Moscow) 1, 137 (1939).

[3]J. Rubinstein, J. Math. Phys. 11, 258 (1970).

[4]M. J. Ablowitz, D. J. Kaup, A. C. Newell, and H. Segur, Phys. Rev. Lett. 30, 1262 (1973).

[5]M. Remoissenet and M. Peyrard, J. Phys. C 14, L481 (1981).

[6]M. Peyrard and M. Remoissenet, Phys. Rev. B 26, 2886 (1982).

[7]M. Peyrard and S. Aubry (unpublished).

[8]M. Peyrard and D. K. Campbell, Physica D (in press).

[9]M. Imada, Institute of Solid State Physics (Tokyo) Technical Report No. ISSP-A-1294, 1983 (unpublished).

[10]R. M. Deleonardis and S. E. Trullinger, Phys. Rev. B 27, 1867 (1983).

[11]A. R. Bishop, Physica 93A, 82 (1978).

[12]G. L. Lamb, *Elements of Soliton Theory* (Wiley, New York, 1980).

[13]D. J. Kaup and A. C. Newell, Phys. Rev. B 18, 5162 (1978).

[14]V. E. Zakharov and A. B. Shabat, Zh. Eksp. Teor. Fiz. 61, 118 (1971) [Sov. Phys.—JETP 34, 62 (1972)].

[15]R. Hirota, J. Math. Phys. 14, 805 (1973).

[16]A. C. Scott, F. Y. F. Chu, and D. W. McLaughlin, Proc. IEEE 61, 1443 (1973).

[17]V. E. Zakharov and A. B. Shabat, Zh. Eksp. Teor. Fiz. 64, 1627 (1973) [Sov. Phys.—JETP 37, 823 (1973)].

[18]C. M. Varma, Phys. Rev. B 14, 244 (1976).

[19]K. Maki and P. Kumar, Phys. Rev. B 14, 3920 (1976); J. Shiefman and P. Kumar, Phys. Scr. 20, 435 (1979).

[20]K. M. Leung, Phys. Rev. B 27, 2877 (1983).

[21]In order to try to increase the probability of a double pair production from a K-$\bar{K}$ collision (nonconservation of particles number), we also tested a model with a *triple*-well periodic potential (period 6π) which can be obtained from Eq. (1.1). In this model three types of kinks exist: types I ($-\pi<\phi<\pi$) and II ($\pi<\phi<3\pi$) correspond to light kinks and type III ($3\pi<\phi<5\pi$) correspond to heavy kinks such that $M_{\rm III}>M_{\rm I}+M_{\rm II}$. Even with this condition $K^{\rm III}$-$\bar{K}^{\rm III}$ collisions failed to produce more than one K-$\bar{K}$ pair ($K^{\rm II}$-$\bar{K}^{\rm II}$).

[22]V. G. Mankankhov, Phys. Rep. 35C, 1 (1978).

[23]T. Sugiyama, Prog. Theor. Phys. 61, 1550 (1979).

[24]D. K. Campbell, J. F. Schonfeld, and C. A. Wingate, Physica D (in press).

[25]Similarly a good prevision of the existence of breathers was also obtained for the model previously studied (see Ref. 6) for positive values of the shape parameter (unpublished).

[26]C. A. Wingate, Ph.D. thesis, University of Illinois, 1978 (unpublished) and SIAM J. Appl. Math. (in press).

[27]M. J. Ablowitz, M. D. Kruskal, and J. F. Ladik, SIAM J. Appl. Math. 36, 478 (1979).

[28]R. Klein, W. Hasenfratz, N. Theodorakopoulos, and W. Wunderlich, Ferroelectrics 26, 721 (1980).

[29]C. A. Condat, R. A. Guyer, and M. D. Miller, Phys. Rev. B 27, 474 (1983); K. M. Leung *ibid.* 26, 226 (1982).

[30]S. C. Ying, Phys. Rev. B 3, 4160 (1971).